Segmenting High-quality Digital Images of Stomata using the Wavelet Spot Detection and the Watershed Transform

Kauê T. N. Duarte, Marco A. G. de Carvalho and Paulo S. Martins
University of Campinas (UNICAMP), School of Technology, R. Paschoal Marmo, 1888, 13484 Limeira, Brazil
kaue.unicamp2011@gmail.com, {magic, paulo}@ft.unicamp.br

Keywords: Stomata, Wavelets, Automatic Counting, Watershed, Image Processing, Image Segmentation.

Abstract: Stomata are cells mostly found in plant leaves, stems and other organs. They are responsible for controlling the gas exchange process, i.e. the plant absorbs air and water vapor is released through transpiration. Therefore, stomata characteristics such as size and shape are important parameters to be taken into account. In this paper, we present a method (aiming at improved efficiency) to detect and count stomata based on the analysis of the multi-scale properties of the Wavelet, including a spot detection task working in the CIELab colorspace. We also segmented stomata images using the Watershed Transform, assigning each spot initially detected as a marker. Experiments with real and high-quality images were conducted and divided in two phases. In the first, the results were compared to both manual enumeration and another recent method existing in the literature, considering the same dataset. In the second, the segmented results were compared to a gold standard provided by a specialist using the F-Measure. The experimental results demonstrate that the proposed method results in better effectiveness for both stomata detection and segmentation.

1 INTRODUCTION

A stoma (also stomate; plural stomata) is a single pore in the epidermis of leaves and other organs in plants that is used to control gas exchange. The size of its opening is regulated by two surrounding guard cells (Willmer and Fricker, 1996). The word stomata means mouth in Greek, due to the fact that it is responsible for the interaction between the internal and external plant environment, and it provides the carbon dioxide and oxygen used in the photosynthesis and respiration. Given that each type of plant has correspondingly a characteristic type of stomata with its own unique size, density and distribution, the detection and analysis of stomata poses a challenge.

Recently, the digital image processing of stomata has received significant attention from researchers in the academia, thus supporting the identification of the level of environmental stress suffered by plants (Laga et al., 2014)(Jian et al., 2011)(Oliveira et al., 2014). For example, the work by (Vialet-Chabrand and Brendel, 2014) addresses the evaluation of stomata density and the authors opt for processing groups of stomata instead of individual ones. In essence, there are several methods that aim at quantifying as well as segmenting the stomata present in plant epidermis.

The human visual perception of the context that we are part of is different from how the computational processes interpret the same type of information. Human beings possess the innate capability of identifying patterns. It is not so straightforward to transfer this capacity to the computational context. However, a simple conversion of the color space to CIELab, as described by Connolly and Fliess (Connolly and Fleiss, 1997), allows the computer to simulate human vision.

Spots are important features within an image context. They usually correspond to bright small objects such as cells that stand out locally in their neighborhood. The application of computational processes to automatically count and segment spots and cells (i.e. stomata in our case) is not a trivial task and it clearly offers the domain experts and field practitioners the needed support to the identification of anomalies. By not employing automatic routines for processing stomata (e.g. counting, segmentation, estimation of density), one must rely on manual procedures which are not always viable due to the amount of time taken (Stepka, 2013). There has been considerable work in the past years dedicated to counting cells on digital biological images (Stepka, 2013; Oliveira et al., 2014; Olivo-Marin, 2002; Lojk et al., 2014; Mallat, 1989; Venkatalakshmi and Thilagavathi, 2013). However, the issue of stomata detection still remains largely an

Duarte K., Carvalho M. and Martins P.
Segmenting High-quality Digital Images of Stomata using the Wavelet Spot Detection and the Watershed Transform.
DOI: 10.5220/0006168105400547
In *Proceedings of the 12th International Joint Conference on Computer Vision, Imaging and Computer Graphics Theory and Applications (VISIGRAPP 2017)*, pages 540-547
ISBN: 978-989-758-225-7

open gap in the literature.

The goal of this paper is to present a technique to count and segment stomata based on the Wavelet Spot Detection and the Watershed Transform. Besides, we also intend to increase the accuracy of the techniques that perform this task. Figure 1 illustrates a high-resolution microscope image (through a combined set of lens) of a Ugni Molinae species, with 40x magnification.

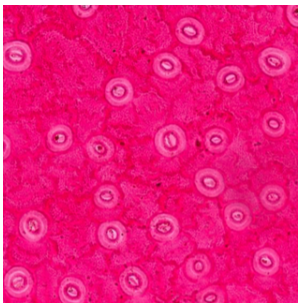

Figure 1: Stomata from *Ugni Molinae Species.*

The remainder of this paper is organized as follows: In Section 2 we review previous work. The proposed approach is described in Section 3. In Section 4 the results are presented and discussed. We summarize and present our conclusions in Section 5.

2 RELATED WORK

Counting cells plays a key role in stomata analysis, and it may include tasks such as segmentation and classification. Within this context, Venkatalakshmi and Thilagavathi (Venkatalakshmi and Thilagavathi, 2013) introduced a method to automatically count red cells (Red Blood Cell Count - RBC), which is used as a means to diagnose health issues in patients. The following steps were defined: 1) Preprocessing, which converts the color space to HSV, and then only uses the S component; 2) Segmentation based on the thresholding of the histogram and on mathematical morphology operators; 3) Combination of the morphological operators, logic and the Hough transform technique to extract the RBC from other cells and from the background; 4) Quantification of the RBC in the image and 5) Definition of the interface for the physician's analysis. The results obtained were compared to manual detection and sent to a doctor for patient analysis.

A general automated approach for detecting and segmenting blood cells of different species was proposed by Karel (Stepka, 2013). His approach can also be directly used in chamber grids. The proposed method comprises of four main steps: 1) preprocessing, consisting of gray level transformation and noise removal by use of Gaussian filtering; 2) use of Hough Transform in order to identify linear structures; 3) finding cell samples; 4) matching between the cell samples and the other cells present in the image by means of correlation. The author provided experimental results that showed good performance in comparison to manual counting.

The method proposed by Oliveira (Oliveira et al., 2014) is used to detect stomata using mathematical morphology. The images used by the authors are from five types of plants. The method consists of the following steps: 1) application of the Gaussian filter; 2) application of the morphology operators *opening-by-reconstruction* and *opening-closing-by-reconstructions*; 3) use the regional minima and 4) elimination of segments that exceed a threshold perimeter value. The results show an average precision around 94%.

Olivo-Marin proposed a new method to detect luminous (bright) points in fluorescent images from biological immunomicroscopy experiments (Olivo-Marin, 2002). The method provides a count of the number of points using the Undecimated Wavelet Transform and Spot Detection. The approach used is to decompose the Wavelet and define, in all levels, the combination of standards, better identifying the spots across different resolutions. The advantage of the method is the satisfactory identification of spots, besides the fact that it may be applied to several types of images.

Lojk (Lojk et al., 2014) proposed a method for automatic and semi-automatic counting in images from fluorescent microscopy. It consists of the following steps: 1) increase of the contrast with the Contrast Limited Adaptive Histogram Equalization algorithm; 2) application of the Otsu Threshold to convert the image to binary format; 3) image segmentation using the Watershed Transform algorithm (allowing cell overlapping), and 4) blob detection. The accuracy of the method was estimated as above 91% in comparison to manual procedures.

Jian (Jian et al., 2011) proposed a remote sensing processing technology using classification. Their goal was to estimate the stomata density of *Populus euphratica* leaves. Their method was defined as follows: 1) Each image is acquired and preprocessing is applied in order to improve visualization. Three specimens are collected from distinct parts of the leaf; 2) Each image is classified using an object-oriented procedure and parameters such as shape, scale and compactness are manually defined; 3) The results are imported into ArcGIS in order to calculate the grid num-

ber for each stomata in all images; 4) The root mean square error is calculated resulting in an accuracy of 98% (of tested samples) in relation to the manual procedure.

Laga (Laga et al., 2014) proposed an supervised approach to stomata detection that measures both their morphologic and structural features. They defined the stomata aperture width as well as guard cell length and width. These parameters are important since they allow a better understanding of water loss associated with the opening and closing of guard cells. The goal was to count the number of stomata and measure their morphological features. The results were obtained from 24 images and were very close to the manual counting. The approach was defined as follows: 1) Image acquisition: It was considered a flag leaf of a wheat plant captured by a "Leica AS LMD" laser dissection microscope; 2) Stomata cell detection, which is based on template fitting. The templates are stored in a database and are distinguished by shape, size and orientation. In this step, the image is preprocessed in order to convert it into a representation that enhances its initial conditions, and thus facilitates stomata detection; 3) Measurement of stomata features: Once the stomata regions have been identified, the method proceeds by measuring the length and width of the stomata aperture and its related guard cells., and 4) Detection refinement: Stomata detection may result in a number of false positives. Because of that, constraints on stomata morphology were used to discard them.

Our work differs from previous works by the following features: 1) Stomata counting: we use the wavelet transform and spot detection (Olivo-Marin, 2002) in order to detect and count stomata in digital images; previous work use different approaches; 2) Spot detection: compared to (Olivo-Marin, 2002), we adapted the wavelet spot detection to work with the detection of dark points instead of bright spots; 3) High-quality images: the set of images adopted in our work were acquired from a high-resolution microscope; 4) CIELab colorspace: the use of this colorspace improves the efficiency of the method, since the a* channel provides better information about the stomata cells, and 5) Watershed Transform: the segmentation process was used to improve the identification of stomata, enabling various future calculations such as stomata area and density.

3 PROPOSED APPROACH

In this section we present the proposed method to detect and segment stomata images. The process consists of three steps: 1) acquisition and extraction; 2) cell detection, and 3) image segmentation. Each step is labeled accordingly in Figure 2 and discussed in turn in the following paragraphs.

3.1 Acquisition and Extraction

A total of 64 images were acquired by a high-precision Hamamatsu Nanozoomer XR microscope (Hamamatsu, 2016) and used in our process. Each image has between 20 and 30 GB and 135168 x 78848 pixels. The initial task was to crop the original image and to analyze each crop individually.

Each image is composed of three channels, i.e. R (red), G(green) and B(blue) (Figure 3,a-c). However, obtaining relevant information through these channels alone is not trivial. Therefore, the conversion of color space from RGB to CIELab is required. Each L*a*b* channel has a distinct meaning: L* represents lightness (0 for black and 100 for white) and a* and b* are chromatic values. This process is carried out in two phases (Connolly and Fleiss, 1997): 1) conversion from RGB to XYZ, and 2) conversion from XYZ to CIELab. The trichromatic space was calculated as follows:

$$X = R*0.4303 + G*0.3416 + B*0.1784 \quad (1)$$

$$Y = R*0.2219 + G*0.7068 + B*0.0713 \quad (2)$$

$$Z = R*0.0202 + G*0.1296 + B*0.9393 \quad (3)$$

The values of L*a*b* were calculated as follows:

$$L^* = 116 f\left(\frac{Y}{Y_0}\right) - 16 \quad (4)$$

$$a^* = 500\left[f\left(\frac{X}{X_0}\right) - f\left(\frac{Y}{Y_0}\right)\right] \quad (5)$$

$$b^* = 200\left[f\left(\frac{Y}{Y_0}\right) - f\left(\frac{Z}{Z_0}\right)\right] \quad (6)$$

where: X_0, Y_0 and Z_0 are the trichromatic values for lightness, which is D50 (see Figure 3 - bottom half, as an example of separate channels L*a*b*).

Through the analysis of each channel independently, we may decide which channel to use in the detection and counting of stomata, i.e. the proposed analysis elicits which channel may allow a better visibility of stomata. In the bottom half of Figure 3 we may clearly identify the center of stomata, which is emphasized in black. Therefore, this is the channel that is used throughout the process.

3.2 Cell Detection

Having extracted the second channel in the CIELab color space, we move on to determine the number of

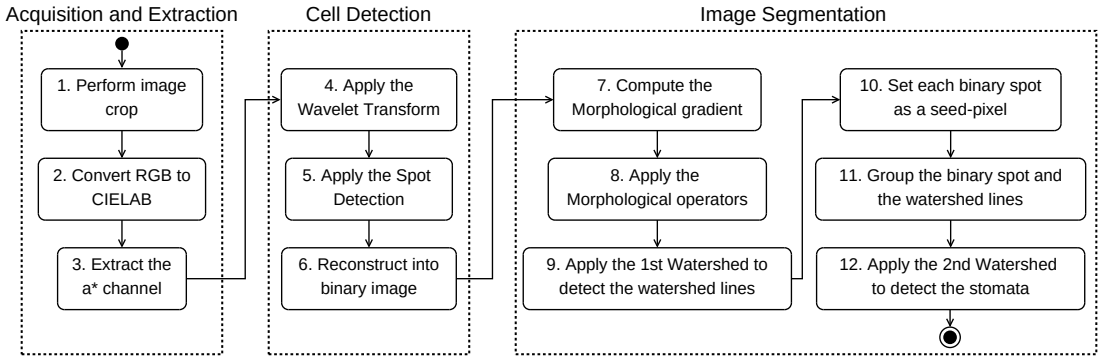

Figure 2: Activity Diagram of the Proposed Approach.

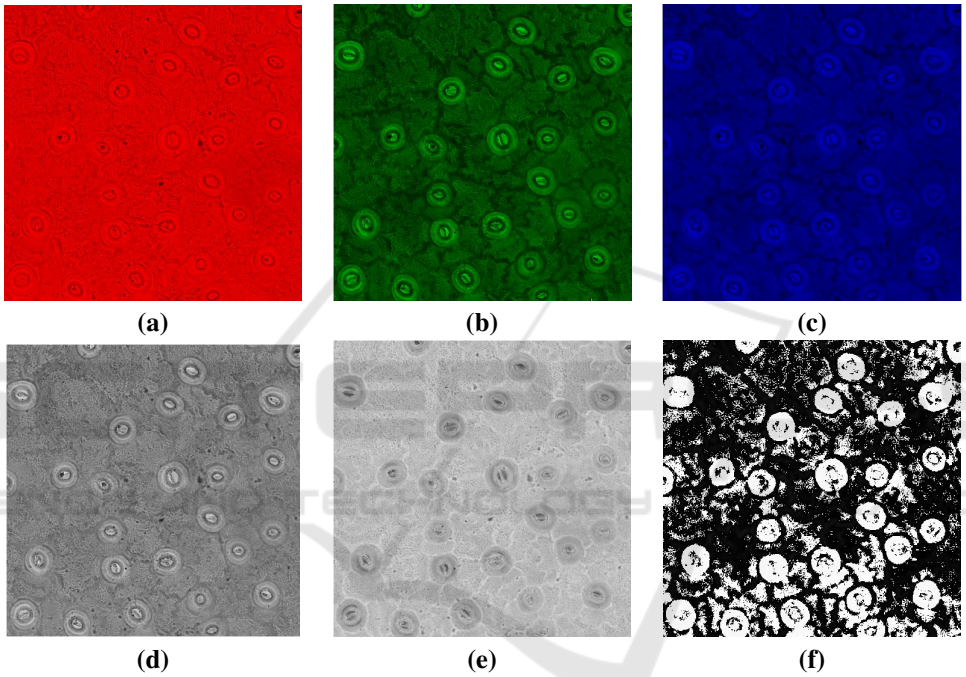

Figure 3: Stomata from *Ugni Molinae Species in RGB to CIELab (a) RGB-channel R; (b) RGB-channel G; (c) RGB-channel B; (d) CIELab-channel L; (e) CIELab-channel a*; (f) CIELab-channel b*.*

stomata cells by applying the Wavelet Spot Detection algorithm (Olivo-Marin, 2002). The Wavelet Transform is based on the "à trous wavelet algorithm", a multi-scale representation where each level i is computed as follows:

$$W_i = A_{i-1}(x,y) - A_i(x,y) \quad (7)$$

where $0 < i \leq J$, A_0(x,y) is the original image, A_i(x,y) is the image after the convolution of A_{i-1}(x,y) with a specific and increased kernel, and J is the number of scales. The W_i(x,y) wavelet coefficients were then filtered out, thus reducing the influence of noise and eliminating the non-significant coefficients. Finally, a correlation image $PJ(x,y)$ is computed by means of the direct product of the wavelet coefficients at all J scales. The spot detection is obtained, therefore, after a thresholding of the PJ(x,y) image. Contrary to existing work which detects the bright points, our work focus on detection of darker spots since they are easier to be identified in the correlation image after the conversion from RGB to CIELab.

3.3 Image Segmentation

After the spot detection analysis, we applied the well-known Watershed Transform, used to find non-uniform image contours. However, we used a slightly adapted method proposed by Meyer (Meyer, 1994). Firstly, we used the a* channel from the converted image to extract a morphological gradient (dilate -

erode), as shown in Figure 4(c). Secondly, it is important to notice that stomata images have texture on their epidermis, what precludes the direct (or immediate) application of the Watershed. Therefore, six morphological operators were applied into the same a* channel prior to the Watershed, in this order: Open, Erode, Reconstruct, Close, Dilate and Reconstruct, using a kernel $k = 2$. These operators were applied to smooth the image.

Figure 4(d-g) illustrates the images resulting from the application of the morphological operators. Then, we applied the first Watershed producing an image with watershed lines. We override the a* channel image with both watershed lines and spots location.

Next, we used a second Watershed to find the regions using the spots as markers, as illustrated in Figure 4(h). Finally, we combined the mask obtained from the previous step with the original image to generate the result shown in Figure 4(i).

4 RESULTS

In this section we present the results divided into two groups: 1) Detection/Counting, and 2) Segmentation. The first group is a necessary (previous) step for the second one. Both counting and segmentation are applied to the same dataset containing 64 image crops (1024 x 1024 pixels each image). The same dataset was used in both studies.

For performance evaluation of the counting and segmentation approaches, we use recall, precision (Baeza-Yates and Ribeiro-Neto, 1999) and the F-Measure (Arbelaez et al., 2011), which are defined as follows:

$$Recall = \frac{TP}{TP+FN} \tag{8}$$

$$Precision = \frac{TP}{TP+FP} \tag{9}$$

$$F = \frac{2 * Recall * Precision}{Recall + Precision} \tag{10}$$

where TP is a true positive, FN is a false negative, and FP is false positive. Note that in segmentation, a TP indicates that a pixel is identified as representing a stoma by both algorithm and gold standard; FN corresponds to the case where the algorithm finds a background pixel whereas the gold standard found a stoma pixel; A FP occurs whenever the algorithm identifies a stoma pixel, but it is in fact a background pixel set by the gold standard.

In counting, a FP occurs when a dot is found in an area where there is no stoma. A single dot found within the actual stoma area represents a TP. Finally, a FN represents the absence of a dot in an actual stoma area.

Table 1 shows a sample with 5 randomly chosen images, retrieved from the 64 image-set that was used in this work. Its purpose is only to convey an idea of how the results were calculated, i.e. the full range of results are actually shown in the following subsection.

4.1 Detection and Counting

In the detection and counting step, we compare our approach with two others methods: 1) manual, considered a gold standard, and 2) the method by Oliveira et al (Oliveira et al., 2014). In order to test the proposed method, we discarded all stomata that were split in two across the center in the cropped image before applying it to the image crops (1024 x 1024 pixels). Those stomata that were only partially cut by the crop (but with the whole center preserved) were considered. The results are shown in Table 1, which compares the performance of the algorithm versus the manual procedure using the recall and precision measures.

In Figure 4(b) we illustrate the results in terms of the stomata identified directly on the image of the plant tissue. As we have mentioned earlier, we used 64 cropped images of the plant (Ugni Molinae), and the results show an improvement over the work by Oliveira (Oliveira et al., 2014). The proposed approach was compared to manual detection for all the samples, and the following results were obtained:

1. *Recall*: The average recall reached by our method was 98.24% against 95.13% obtained by Oliveira (Oliveira et al., 2014). Furthermore, recall was improved upon the latter work in 84.37 % of the images.
2. *Precision:* The average precision reached by the proposed method was 98.34% against 92.81 % from Oliveira (Oliveira et al., 2014). Moreover, compared to the latter work, the proposed method showed a more satisfactory precision in 90.62% of images.
3. *F-Measure:* The average F-Measure found by our method was 98.25% against 93.80% from Oliveira (Oliveira et al., 2014). It is also important to notice that 84.37% of images scored an improved F-measure in comparison to latter work. The graph shown in Figure 5 illustrates the comparison of the methods for each image using the F-Measure.

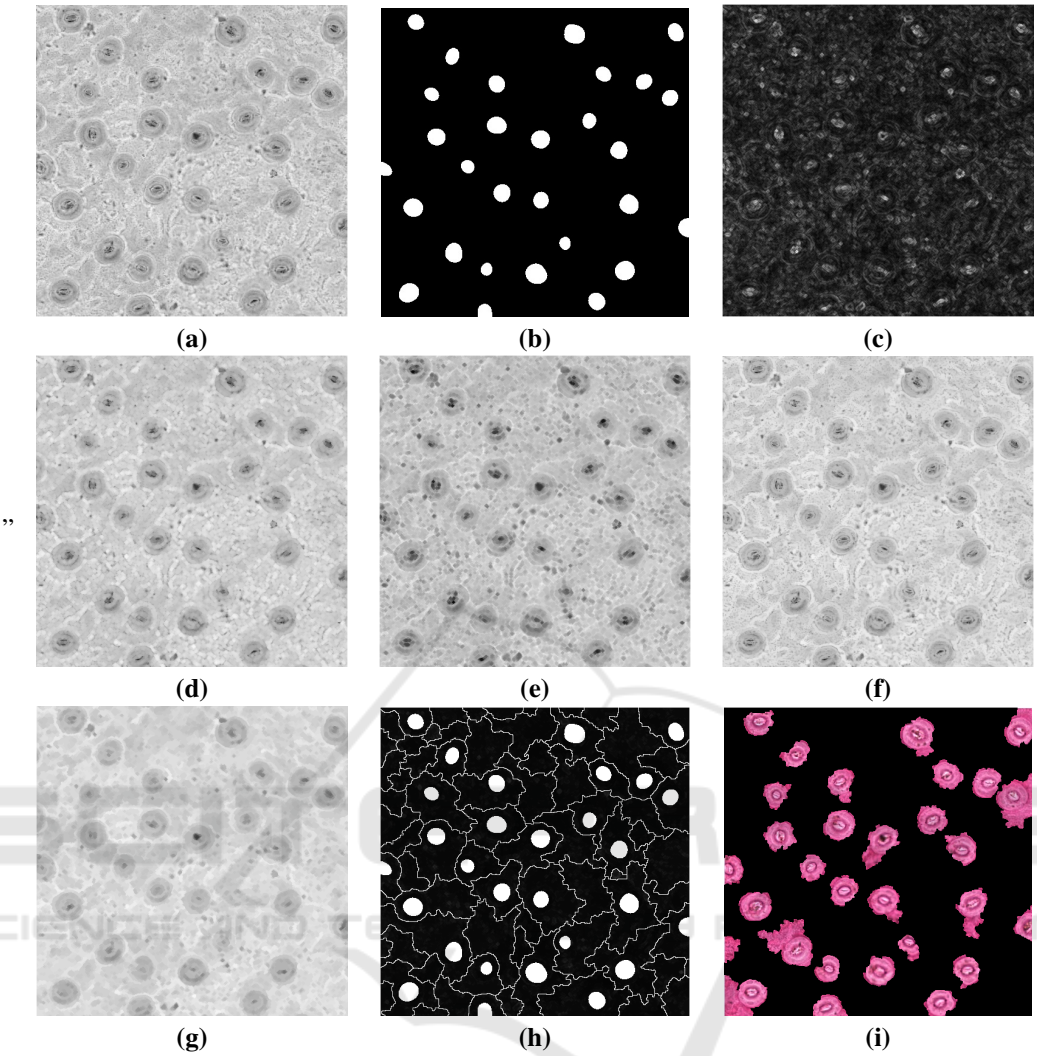

Figure 4: Stomata Segmentation Process from *UgniMolinae* Species (a) Channel a* ; (b) Binary spots from Wavelet Spot Detection; (c) Morphological Gradient; (d) Open; (e) Erode; (f) Reconstruct; (g) Close; (h) Watershed lines and spots; (i) Stomata detected. The images (a) and (c-g) had their contrast enhanced for better visualization.

4.2 Segmentation

The segmented image was compared to the gold standard pixel by pixel. For the test, we also discarded all split stomata that occur during the crop process. The gold standard was prepared by a specialist using the Interactive Segmentation Tool (McGuinness and O'Connor, 2010), and then compared using the F-Measure.

This new approach reaches an F-Measure of 70%. Figure 6 shows a graph that represents the relationship between Recall, Precision and F-Measure for each tested image.

5 SUMMARY AND CONCLUSION

The analysis of stomata count is a crucial activity in the assessment of plants and the state-of-the-art in this field is still limited. In this work we introduced a new method for detection/counting and segmentation of stomata using the conversion of the color space, the Nondecimated Wavelet Transform for the detection of dark spots (i.e. stomata), and the Watershed Transform. We conducted experiments with high quality digital images and the results obtained indicated a satisfactory determination of the number of stomata in the tissue. The first case of the comparison analysis showed that our approach provided precision and re-

Table 1: Performance analysis of the proposed approach in comparison to the gold standard. N_h is the number of stomata detected by the specialist; N_a represents the number of stomata detected automatically; FP is the number of false positives; FN is the number of false negatives; P is the Precision; R represents Recall; F is the F-Measure.

Image	Manual	Our Method							Oliveira (2014)						
#	Nh	Na	TP	FP	FN	R	P	F	Na	TP	FP	FN	R	P	F
1	27	29	27	2	0	93.1	100	96.4	30	25	5	2	83.3	92.6	87.7
2	24	23	23	0	1	100	95.8	97.8	21	20	1	4	95.2	83.3	88.8
3	21	21	21	0	0	100	100	100	23	20	3	1	86.9	95.2	90.8
4	23	24	23	1	0	95.8	100	97.8	25	23	2	0	92	100	95.8
5	25	27	25	2	0	92.6	100	96.1	20	20	0	5	100	80	88.8

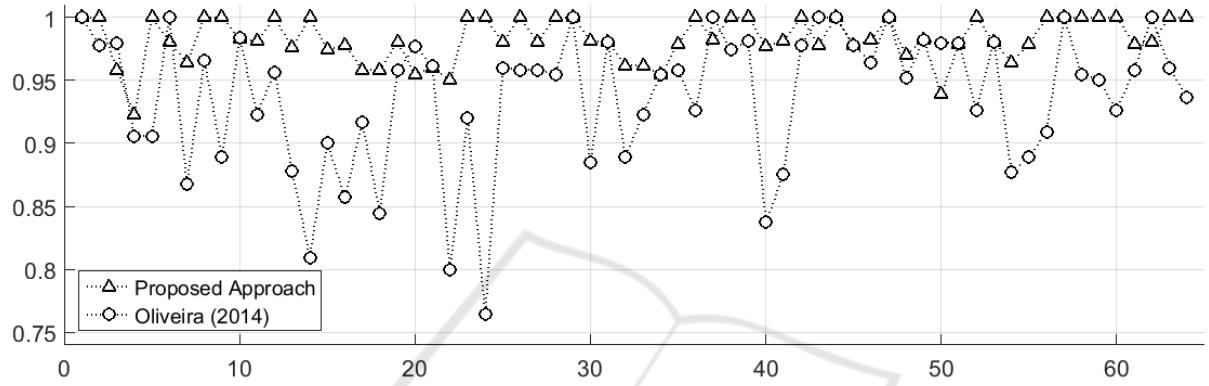

Figure 5: Comparison Analysis by F-Measure for 64 images: Detection/Counting.

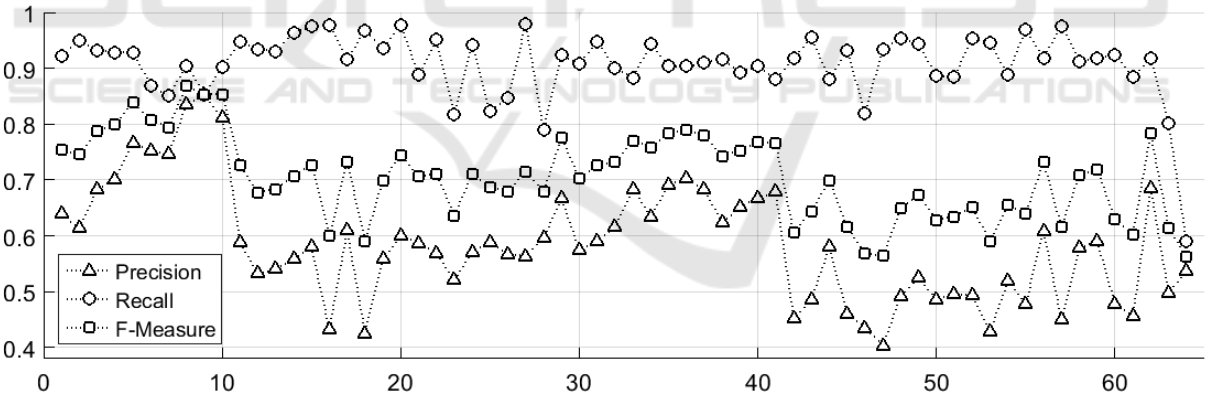

Figure 6: Performance evaluation of segmentation for 64 stomata images: Segmentation.

call values (84.37% and 90.62% respectively) larger than previous work and comparable in performance to manual, non-automatic counting. The second case indicated an F-Measure of 70 % in comparison to manual segmentation.

As future work, we will focus on a new approach to count the stomata that were split in the image-cropping process, in order to further improve precision. Deep Learning could be a future approach to be applied, depending on the improvement of our dataset, e.g. regarding a larger number of images. We also aim at image segmentation using Spectral Graph Theory (SGT) and Normalized Cut with texture analysis and comparison with the proposed approach, as well as the computation of additional information about stomata such as area, aperture width, guard-cells width and length.

ACKNOWLEDGEMENTS

The authors would like to thank SCIANLab from the University of Chile for providing the images of vegetable tissue used in this work.

REFERENCES

Arbelaez, P., Maire, M., Fowlkes, C., and Malik, J. (2011). Contour detection and hierarchical image segmentation. *IEEE Transactions on Pattern Analysis and Machine Intelligence*, 33(5):898–916.

Baeza-Yates, R. A. and Ribeiro-Neto, B. (1999). *Modern Information Retrieval*. Addison-Wesley Longman Publishing Co., Inc., Boston, MA, USA.

Connolly, C. and Fleiss, T. (1997). A study of efficiency and accuracy in the transformation from rgb to cielab color space. *IEEE Transactions on Image Processing*, 6(7):1046–1048.

Hamamatsu (2016). Hamamatsu Nanozoomer XR microscope. http://www.hamamatsu.com/eu/en/community/nanozoomer/index.html. [Online; accessed 21-September-2016].

Jian, S., Zhao, C., and Zhao, Y. (2011). Based on remote sensing processing technology estimating leaves stomatal density of populus euphratica. In *Geoscience and Remote Sensing Symposium (IGARSS), 2011 IEEE International*, pages 547–550.

Laga, H., Shahinnia, F., and Fleury, D. (2014). Image-based plant stomata phenotyping. In *Control Automation Robotics Vision (ICARCV), 2014 13th International Conference on*, pages 217–222.

Lojk, J., Sajn, L., Aibej, U., and Pavlin, M. (2014). Automatic cell counter for cell viability estimation. In *Information and Communication Technology, Electronics and Microelectronics (MIPRO), 2014 37th International Convention on*, pages 239–244.

Mallat, S. G. (1989). A theory for multi-resolution signal decomposition: the wavelet representation. *IEEE Transactions on Pattern Analysis and Machine Intelligence*, 11(7):674–693.

McGuinness, K. and O'Connor, N. E. (2010). A comparative evaluation of interactive segmentation algorithms. *Pattern Recognition*, 43(2):434–444.

Meyer, F. (1994). Mathematical morphology and its applications to signal processing topographic distance and watershed lines. *Signal Processing*, 38(1):113 – 125.

Oliveira, M. C. S., Silva, N. R., Casanova, D., Pinheiro, L. F. S., Kolb, R. M., and Bruno, O. M. (2014). Automatic counting of stomata in epidermis microscopic images. In *X Workshop de Visão Computacional*.

Olivo-Marin, J.-C. (2002). Extraction of spots in biological images using multiscale products. *Pattern Recognition*, 35(9):1989 – 1996.

Stepka, K. (2013). *Image Analysis: 18th Scandinavian Conference, SCIA 2013, Espoo, Finland, June 17-20, 2013. Proceedings*, chapter Automated Cell Counting in Bürker Chamber, pages 236–245. Springer Berlin Heidelberg, Berlin, Heidelberg.

Venkatalakshmi, B. and Thilagavathi, K. (2013). Automatic red blood cell counting using hough transform. In *Information Communication Technologies (ICT), 2013 IEEE Conference on*, pages 267–271.

Vialet-Chabrand, S. and Brendel, O. (2014). Automatic measurement of stomatal density from microphotographs. *Trees*, 28(6):1859–1865.

Willmer, C. and Fricker, M. (1996). *Stomata*. Topics in plant functional biology. Springer.